

ROBUST CONTROL ANALYSIS USING REAL-TIME IMPLEMENTATION OF A HYBRID FUEL CELL POWER GENERATION SYSTEM

D. HERNANDEZ-TORRES^{1,2}, D. RIU¹, O. SENAME², F. DRUART³

¹G2ELab, ²GIPSA-Lab, ³LEPMI Lab, France,

Delphine.Riu@g2elab.grenoble-inp.fr

ABSTRACT

In this paper a complete robustness analysis is performed for a hybrid Fuel Cell/Supercapacitor generation system with power management, realized through the control of two identical boost power converters. For the closed-loop control a previously proposed multivariable robust control is considered. The robust control strategy analyzed consists of a multivariable Proportional-Integral controller found using an algorithm with a Linear Matrix Inequalities (LMI) formulation proposed by the authors in former works. The control actuators are the duty cycles of the boost power converters interfacing the Fuel Cell (FC) and the Supercapacitor (SC) with the system electrical load. The control effectively achieves stability and performance robustness for several considered parameter variations sets. Simulation results were obtained using μ -analysis theory and the experimental validation was achieved. The results obtained show the improvement of the system robustness with a strategy that can be generalized as a robust control methodology.

1. INTRODUCTION

The control and energy management of FC systems with secondary energy storage devices is a major challenging problem. When the FC auxiliary systems are considered the problem becomes more complex. Little attention has been given to robust control strategies and robustness analysis to hybrid generation systems using FC. The work presented in this paper deals with the robustness analysis of a control strategy presented by the authors in previous works [1-3]. The proposed controller consists of a multivariable PI controller computed using an algorithm with LMI formulation and H_∞ performance specification. This algorithm was originally proposed by [4]. A simplified version of the algorithm for the hybrid FC system was presented in detail in [1]. The hybrid system is composed by a PEMFC and a SC each one interfaced by two identical parallel-connected boost converters. For the robustness study μ -analysis is used, see [5] for a detailed review in μ theory. Some robustness results obtained with the proposed methodology were previously compared to those obtained using classic control strategies for this type of system, see [1]. In classic control the multi-loop strategy is commonly used [6-7]. In this paper the robust controller performances obtained by simulation using μ -analysis are validated by experimental results using a real-time implementation of the hybrid system. A sensitivity analysis is performed to study the system relationship with physical parameter variations and its participation factors. Finally, a preliminary system component design procedure using the results obtained in the robustness analysis is presented. The limitations of this procedure are identified and discussed.

2. STUDIED SYSTEM

The studied system is composed by a 1kW PEMFC and a 58F-15V SC each one interfaced by two identical boost converters that rise up the utilization voltage to 24V. The hybrid source was designed by [8] for a FC residential power supply application. The SC recharge is assured by a third converter, a flyback converter, that draws some power directly from the FC and whose control is assumed to be perfect. The SC recharge was designed to operate only when no current is being drawn from the SC. There are several other possible converter configurations including the use of a reversible boost converter to recharge the SC. The coordination of several power converter control configurations and FC system considerations are presented in [9]. The studied hybrid configuration is presented in Figure 1. The FC model used combines the dynamic performance, by a simplified electrical equivalent circuit modeling, with the static polarization curve characteristic. The model scheme is presented in Figure 2. For the real-time experimentation an emulation of the FC dynamic was implemented to avoid damage on the real FC during tests. The model used for the emulator is the same model shown in figure 2, sending a 0-10V control signal to a voltage-controlled DC source. The FC static polarization curve and its respective power curve are presented in Figure 3.

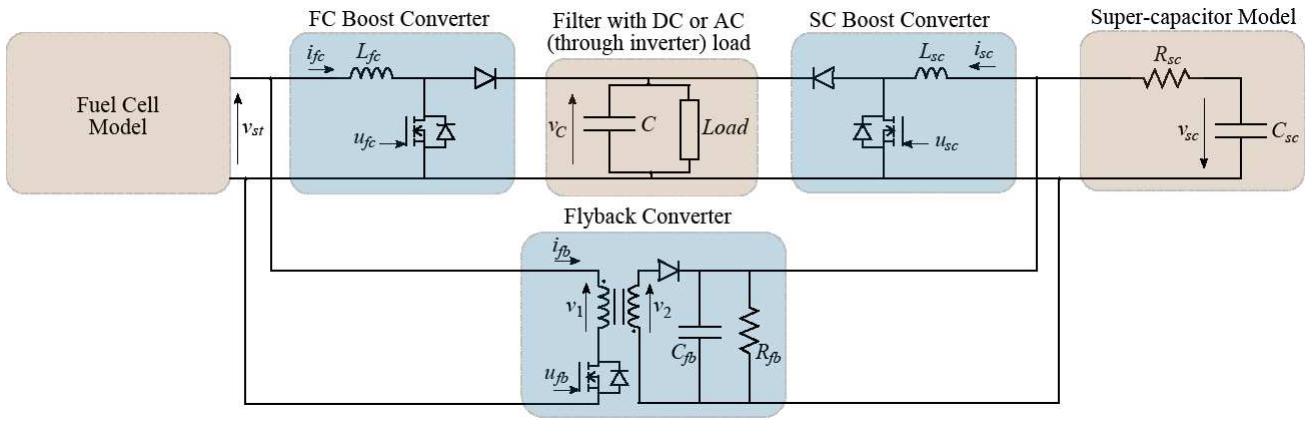


Figure 1. Hybrid FC/SC system configuration

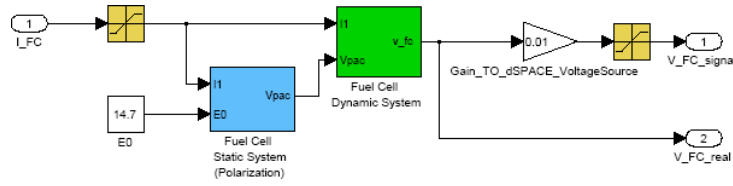


Figure 2. Fuel cell model used for simulation and emulation in the real-time implementation

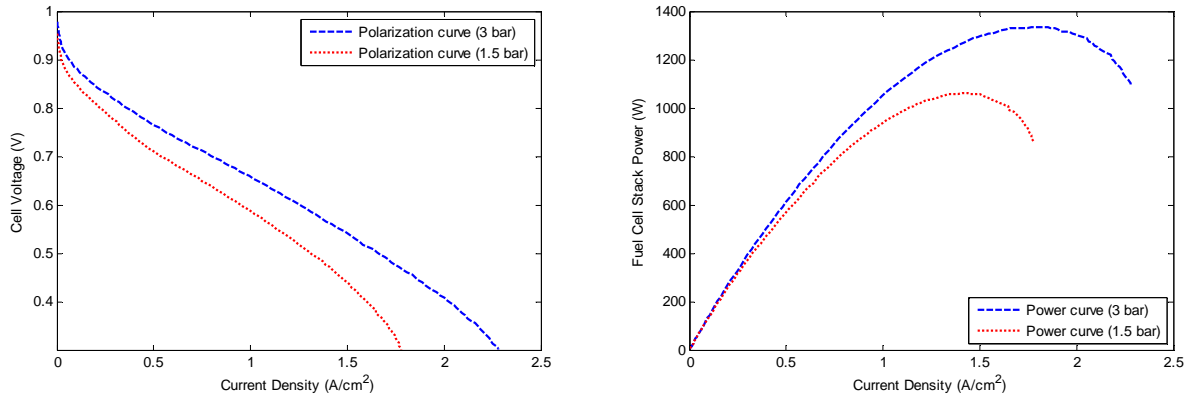


Figure 3. Static polarization characteristic (left) and the FC power curve (right)

2.1 Hybrid System Model

Average modeling is used to describe the dynamic equation of the hybrid power generation system. The non-linear average model of the system is given by the following set of equations:

$$\begin{aligned} \frac{dV_{C_c}}{dt} &= \frac{1}{C_c} \left[I_1 - \frac{V_{C_c}}{R_{tc}} \right] \\ \frac{dV_{C_a}}{dt} &= \frac{1}{C_a} \left[I_1 - \frac{V_{C_a}}{R_{ta}} \right] \\ \frac{dI_1}{dt} &= \frac{1}{L_1} [E_0 - V_{C_a} - V_{C_c} - R_m I_1 - (1 - \alpha_1) V_C] \\ \frac{dI_2}{dt} &= \frac{1}{L_2} [V_{sc} - R_2 I_2 - (1 - \alpha_2) V_C] \\ \frac{dV_{sc}}{dt} &= \frac{1}{C_{sc}} I_2 \\ \frac{dV_C}{dt} &= \frac{1}{C} \left[(1 - \alpha_1) I_1 + (1 - \alpha_2) I_2 - \frac{V_C}{R} \right] \end{aligned} \quad (1)$$

(1)

In this model the state variables are V_{C_c} the double layer capacitor in the FC cathode, V_{C_a} the double layer capacitor in the FC anode, I_1 the FC output current, I_2 the SC output current, V_{sc} the SC voltage and V_C the output filter capacitor voltage. The control inputs are α_1 and α_2 , the average values of the switching functions of the FC and SC power converters.

The linearized average model is given by:

$$\begin{aligned} \Delta \dot{x} &= \hat{A} \Delta x + \hat{B}_1 \Delta \omega + \hat{B}_2 \Delta u \\ \Delta x &= [\Delta V_{C_c} \quad \Delta V_{C_a} \quad \Delta I_1 \quad \Delta I_2 \quad \Delta V_{sc} \quad \Delta V_C]^T \\ \Delta u &= \Delta \alpha_1, \Delta \omega = \Delta P_{ch} \end{aligned} \quad (2)$$

with:

$$\hat{A} = \begin{bmatrix} -\frac{1}{R_{tc}C_c} & 0 & \frac{1}{C_c} & 0 & 0 & 0 \\ 0 & -\frac{1}{R_{ta}C_a} & \frac{1}{C_a} & 0 & 0 & 0 \\ -\frac{1}{L_1} & -\frac{1}{L_1} & -\frac{R_m}{L_1} & 0 & 0 & -\frac{(1-\alpha_{1e})}{L_1} \\ 0 & 0 & 0 & -\frac{R_2}{L_2} & \frac{1}{L_2} & -\frac{(1-\alpha_{2e})}{L_2} \\ 0 & 0 & 0 & -\frac{1}{C_{sc}} & 0 & 0 \\ 0 & 0 & \frac{(1-\alpha_{1e})}{C} & \frac{(1-\alpha_{2e})}{C} & 0 & -\frac{1}{RC} \end{bmatrix}$$

$$\hat{B}_1 = \begin{bmatrix} 0 & 0 & 0 & 0 & 0 & \frac{V_{ce}}{R^2} \end{bmatrix}^T, \hat{B}_2 = \begin{bmatrix} 0 & 0 & \frac{V_{ce}}{L_1} & 0 & 0 & -\frac{I_{1e}}{C} \end{bmatrix}^T$$

Physical parameters of the system are given by : $E_0 = 13,4V$, $R_m = 1,28e-3\Omega$, $R_{tc} = 2,04e-3\Omega$, $R_{ta} = 4,72e-4\Omega$, $C_a = C_c = 2,12F$, $C_{sc} = 58F$, $R_{sc} = 0,019\Omega$, $L_1 = 50\mu H$, $L_2 = 50\mu H$, $C = 37,6mF$, $R = 1,2126\Omega$.

2.2 Eigenvalue Sensitivity Analysis

The theory of eigenvalues and eigenvectors sensitivity and participation factors is well described under the small signal stability analysis chapter in [10]. The sensitivity matrix describes the perception of variation ($\partial\lambda_i/\partial a_{kj}$) of a eigenvalue λ_i as a function of the elements of the state-space matrix **A**. The analysis of each eigenvalue sensitivity matrix lead to the following comments. The mode 1 (the left most eigenvalue located at -990) is influenced by the double layer capacitances (C_{dl}) of the FC model. The mode 2 (a first complex conjugated pair with the real part located at -116) is influenced by both C_{dl} and C the DC bus filter capacitance. The mode 3 (a second complex conjugated pair with the real part located at -217) is influenced by the value of C . Finally the mode 4 (a real eigenvalue located at -0.73) is highly influenced by the SC value. However, even with a slight influence on modes 1 and 4, it can be concluded from this analysis that capacitance C has a dominant influence on all the system modes. The participation factors matrix gives a measure on the participation of the k -th state variable in the i -th mode. The participation factors matrix is presented in Table 1.

Table 1. Participation factors.

Participation factors						
	Mode 1	Mode 2		Mode 3		Mode 4
V_{C_c}	0.0001	0.0074	0.0074	0.5059	0.5059	0.0003
V_{C_a}	1.0074	0.0023	0.0023	0.0040	0.0040	0.0000
I_1	0.0078	0.2737	0.2737	0.2589	0.2589	0.0019
I_2	0.0004	0.2759	0.2759	0.2967	0.2967	0.0015
V_{sc}	0.0000	0.0003	0.0003	0.0020	0.0020	1.0030
V_C	0.0007	0.5396	0.5396	0.0438	0.0438	0.0001

This means that modes 1 and 3 are affects the double layer capacitor voltage, the mode 2 affects de DC bus voltage V_C and the mode 4 affects the SC voltage dynamic.

3. ROBUST CONTROL

The robust control strategy developed is based on multivariable PI control considering H_∞ performance, the controller computation along with the respective analysis was presented by the authors in previous works [1-3]. An important tool used for the control synthesis is the formulation of the problem in the form of Linear Matrix Inequalities (LMI). Furthermore, an iterative version of this tool developed in [4] to solve de MIMO PI control problem is considered. The system model presented before is arranged in the following form:

$$\begin{aligned} \dot{x} &= Ax(t) + B_1\omega(t) + B_2u(t) \\ z(t) &= C_1x(t) + D_{11}\omega(t) + D_{12}u(t) \\ y(t) &= C_2x(t) + D_{21}\omega(t) \end{aligned} \quad (3)$$

The system in (3) includes the performance specifications on the performance output $z(t)$ in the form of frequency weighting functions [5]. These functions are in the form:

$$\frac{1}{W_e} = \frac{s + \omega_B A}{s/M + \omega_B} \quad \frac{1}{W_u} = \frac{A_u s + \omega_{bc}}{s + \omega_{bc}/M_u} \quad (4)$$

The output measurements $y(t)$ are the DC bus voltage V_C and the FC current. The load current is considered as the system external perturbation $\omega(t)$. After the solution of the optimization problem a MIMO PI controller is obtained. The sensitivity along with the complementary sensitivity and weighting functions of the closed-loop system are presented in Figure 4.

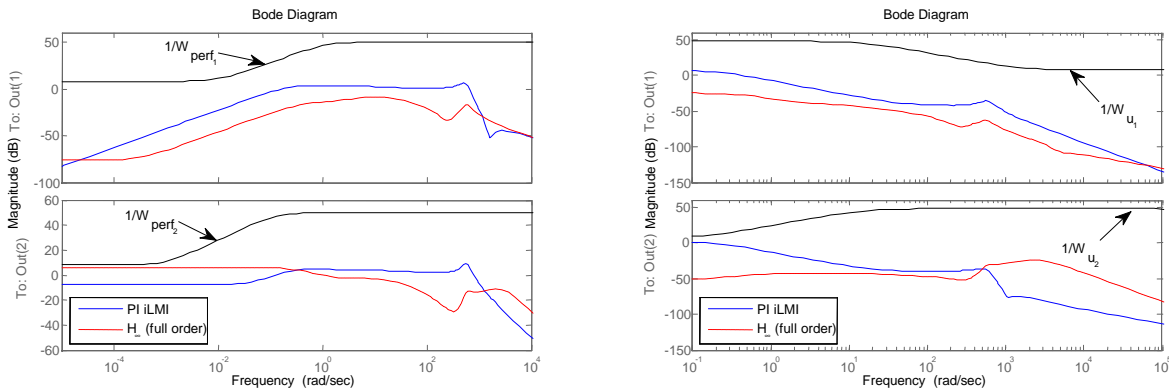


Figure 4. Sensitivity and complementary sensitivity of the closed-loop system

4. ROBUSTNESS ANALYSIS

The theory behind the robustness analysis considered in this paper is based on the computation of the system structured singular value (μ value). However, the unstructured multiplicative input model is used to represent uncertainties. Robust stability and robust performance are considered. The μ value is computed for the different found controllers under the general control configuration forms. In the case of the studied hybrid system, uncertainties are given in first place by the electrical system parameters (inductances, capacitors and resistances), but are also representative of variations in the FC stack polarization curves as a consequence of degradation of cells. They could also represent slight changes in the FC humidification or temperature.

4.1 Parametric uncertainties

In this paper, variations on the hybrid system physical parameters are considered. Resistance variations are a consequence of possible variations in the temperature, in addition to the component tolerance. Using a linear approximation of the resistance variation with temperature, an estimated $\pm 25\%$ variation in the value of

resistances is considered. In the case of capacitors according to several manufacturers, a capacitor tolerance varies between $\pm 10\%$ and $\pm 20\%$ the nominal value of the capacitor. In this paper a scenario with a $\pm 10\%$ variation in the capacitor value is considered. Resistances, inductances and SC values may vary significantly during different loading and temperature conditions [11]. Even when a maximum variation of 20% in the loading conditions was considered, a pessimistic variation of 40% in the system inductances is studied. In the case of the SC different loading conditions are considered by taking different states of charge (SOC) of the SC. The SOC_{SC} is defined by:

$$SOC_{SC} = \left(\frac{v_{intSC}}{v_{maxSC}} \right)^2 \quad (5)$$

With v_{intSC} being the internal SC voltage and v_{maxSC} the maximum possible SC voltage. This could lead to a capacitance variation of as much as -40% and $+10\%$. The weighting functions obtained with these parametric variations to model complex uncertainties are presented in Figure 5.

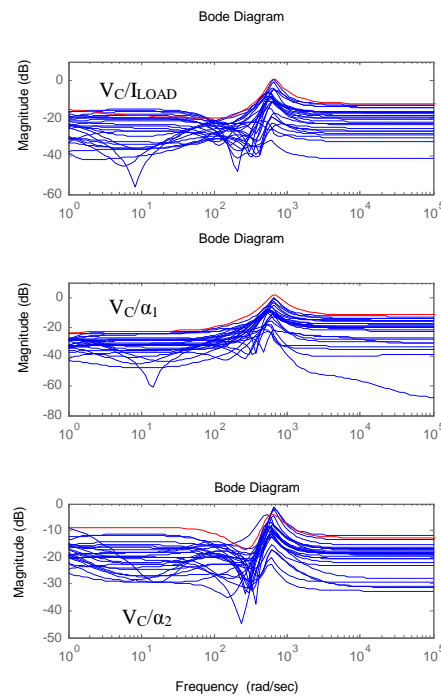


Figure 5. Weighting functions to model complex uncertainties

4.2 μ -Analysis

The robust stability and the robust performance plots are presented in Figure 6. In this case a full order H_∞ controller is also considered for comparison. As shown in the figure, both controllers achieve robust stability and robust performance for the uncertainties levels defined before.

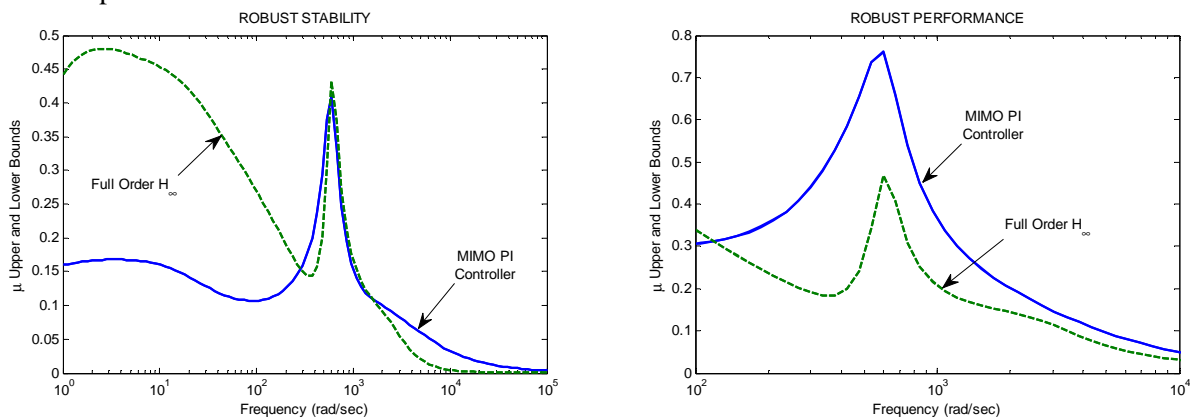


Figure 6. Robust stability (left) and robust performance (right) plots

5. REAL-TIME IMPLEMENTATION

The test-bench is composed by a 1kW Paxitech© PEM Fuel Cell and a 58F Maxwell© super-capacitor. As said before however, the FC dynamic was emulated by a Xantrex© 100-60 DC programmable source and a Simulink/dSPACE real-time environment. Under normal loading conditions, at approximately 475W, the flyback converter will draw 0.4A to keep the SC charge at a nominal voltage of 14.5V in the SC. A small auxiliary 12V battery is used to power the control boards for the boost converters, generating the necessary PWM signals. The PWM is fixed at 50kHz. A DS1104 dSPACE real-time control board is used to capture the system currents and voltage and to send the 0–5V control signal for the PWM (duty cycle). The arrangement of the power converters is presented in Figure 7.



Figure 7. Arrangement of power converters in the test-bench setup

The temperature evolution from an ambient temperature of 25°C after a continuous 1h operation (at nominal loading conditions) of the converters arrangement shown before is presented in Figure 8. Then, experimental results are presented for $\pm 5\%$, $\pm 10\%$ and $\pm 20\%$ load steps.



Figure 8. Temperature of the power converters after 1h operation at rating load

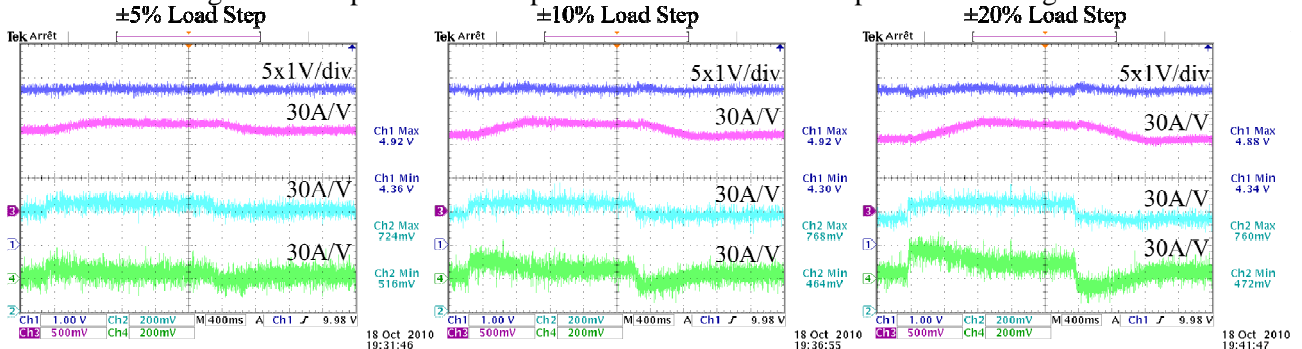


Figure 9. Experimental results (Ch1: V_C , Ch2: I_{LOAD} , Ch3: I_1 , Ch4: I_2)

These results are compared in Figures 10 with the simulation results obtained from the non-linear average model of the closed-loop system.

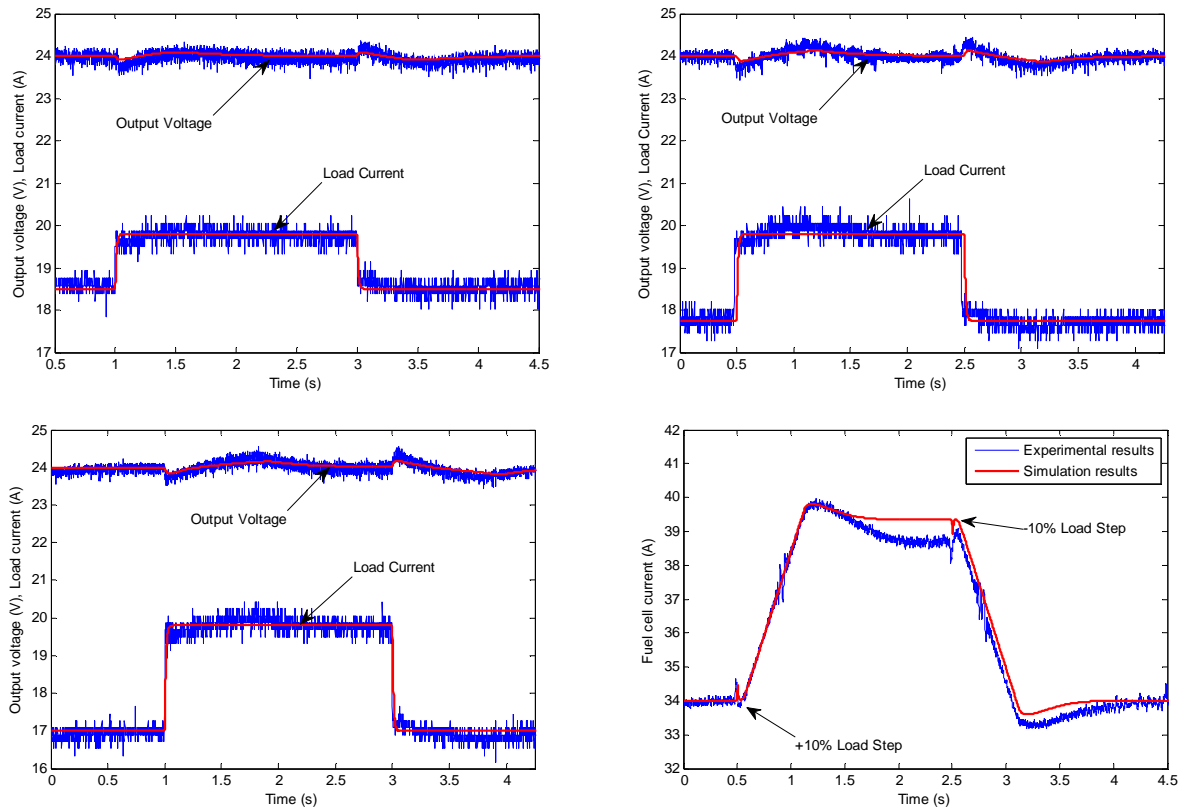


Figure 10. Comparison with simulations results for $\pm 5\%$ (top-left), $\pm 10\%$ (top-right), $\pm 20\%$ (bottom-left) and the fuel cell current (bottom-right) for $\pm 10\%$ load steps.

The experimental results show the effectiveness and robustness of the control methodology for several loading conditions. The controlled output DC bus voltage remains within the desired margins ($\pm 10\%$). Several tests were also performed for different SOC_{SC} values. In Figure 11 the results for $\pm 10\%$ load steps and SOC_{SC} values of 0.5 and 0.75 are presented. In this case a SOC_{SC} of 0.5 was found to be the minimum possible value for the hybrid system under study. As before, the control strategy is able to keep desired performances on the output DC bus voltage and the FC current, validating the results obtained in the μ -Analysis.

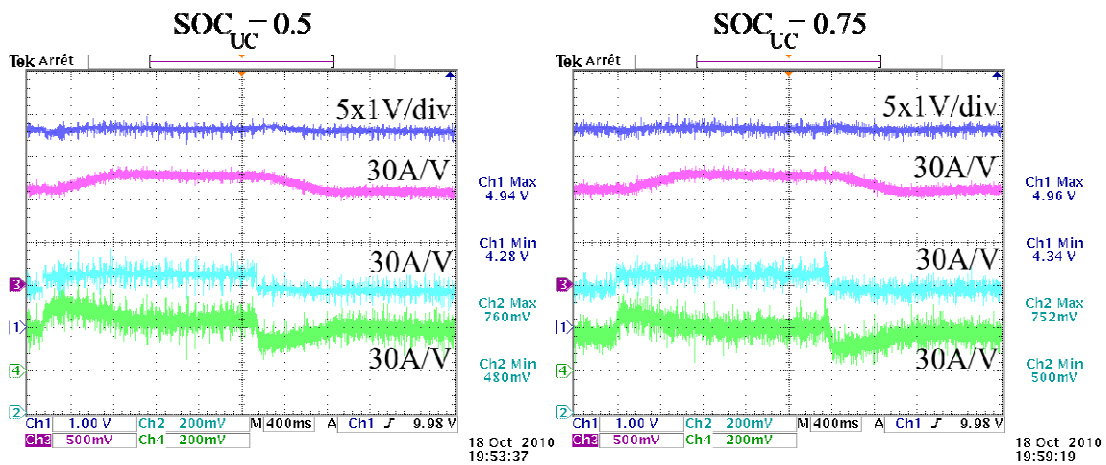


Figure 11. Experimental results for several SOC_{SC} values (Ch1: V_C , Ch2: I_{LOAD} , Ch3: I_1 , Ch4: I_2)

6. COMPONENT DESIGN AFTER ROBUSTNESS

In the design process of the hybrid system power management a dedicated tool that considers the final complete system performance from the beginning of the design process could be very interesting. The system components variations are then defined as the parametric uncertainties. In order to account for the performance specifications parameters influence on system robustness, several pareto curves were traced for variations on the DC bus filter capacitance. With the single parameter variation defined as:

$$q_p = q_{NOM} (1 + k_q p_q \Delta) \quad (6)$$

with q_{NOM} the nominal value of the parameter and p_q the parameter variation, a new parameter, the “robustness factor”, defines the deviation from the fixed parameter variation level. In Figure 12 the curves for the maximum peak magnitude (top-left) and the closed-loop bandwidth (top-right) are presented. These curves corresponds to variations in the DC bus capacitor value and the robustness factor is the maximum level of allowable parameter variation to guarantee robust performance ($\mu=1$). The robustness factor gives the level of variation for the capacitance C and the difference between this capacitance and the nominal value is defined as the gain. As the relation between the volume and the value of the capacitance is linear, this could be translated into a gain in volume. For the specific case of the hybrid system treated this gain is around 1800cm^3 , proving the contribution of the robust control strategy to component design. Of course, the limitation of the desired filter frequency value and the capacitor satisfying this frequency should be respected. However as a limitation in this procedure it can be said that it cannot be applied to the sizing of the SC for example, since the natural frequency of SC are lower than 1Hz, far from the natural frequency of the DC bus filter.

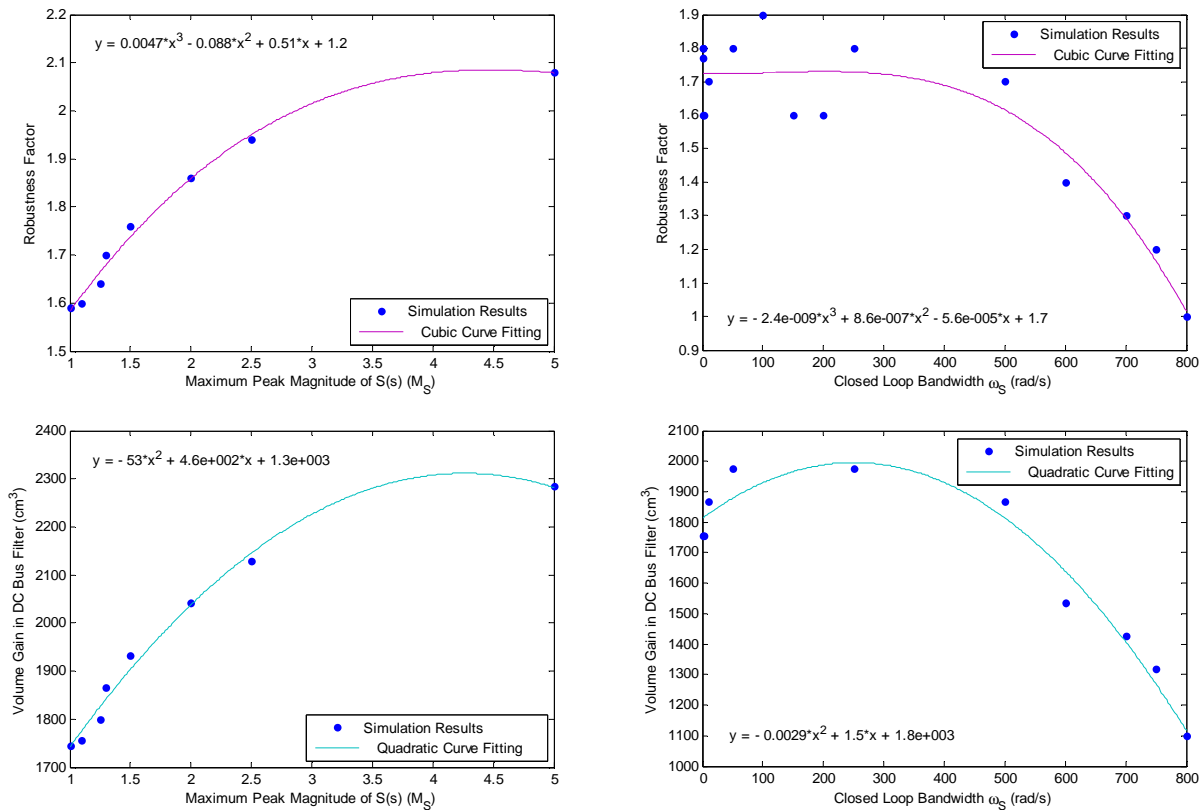


Figure 12. Pareto curves for component design

CONCLUSION

The experimental results in this paper show the effectiveness of the control strategy under several uncertain conditions. The controller optimization, the robustness analysis and the preliminary procedure for system component sizing are all presented aiming towards a generalized control strategy that goes from the system conception and design onto the real implementation. It was shown, however, that as a limitation to the strategy, the sizing of the auxiliary power source is not possible under the presented form of the methodology.

REFERENCES

1. Hernandez-Torres D., Riu D., Sename O., and Druart F., 2010, On the robust control of DC-DC converters: Application to a hybrid power generation system, presented in *4th IFAC Symposium on System, Structure and Control*.
2. Hernandez-Torres D., Riu D. and Sename O., 2010, Design and Experimental Validation of a Robust Control Method for a Hybrid Fuel Cell Power Generation System, presented in the *IEEE Energy Conversion Congress & Expo ECCE 2010*.
3. Hernandez-Torres D., Riu D., Sename O. and Druart F., 2010, Robust Optimal Control Strategies for a Hybrid Fuel Cell Power Management System, Accepted for publication in the *IEEE 36th Annual Conference of the IEEE Industrial Electronics Society IECON 2010*.
4. He Y. and Wang Q.-G., 2006, An improved iLMI method for static output feedback control with application to multivariable pid control, *IEEE Trans. on Automatic Control*, vol. 51, pp. 1678–1683.
5. Skogestad S. and Postlethwaite I., *Multivariable Feedback Control: Analysis and Design*, 1996, *John Wiley & Sons*, New York.
6. Middlebrook, R.D., 1987, Topics in multiple-loop regulators and current-mode programming, *IEEE Trans. on Power Electronics*, vol. 2, n°2: pp. 109–124.
7. Alvarez-Ramirez, J., Cervantes, I., Espinosa-Perez, G., Maya, P., and Morales, A., 2001, A stable design of PI control for DC-DC converters with an RHS zero. *IEEE Trans. on Circuits and Systems I: Fundamental Theory and Applications*, vol. 1, n°48: pp. 103–106.
8. Sailler, S., *Générateurs Electrochimique et Stokage Ilôtés*, 2008, *PhD thesis from the Institute Polytechnique de Grenoble (in french)*, Grenoble.
9. Pera, M., Candusso, D., Hissel, D., and Kauffmann, J., 2007, Power generation by fuel cells. *IEEE Industrial Electronics Magazine*, vol. 1, n°3: pp. 28–37.
10. Kundur P., *Power System Stability and Control*, 1994, *McGraw-Hill Inc.*, New York.
11. Gualous H., Bouquain D., Berthon A., Kauffmann J.M., 2003, Experimental study of supercapacitor serial resistance and capacitance variations with temperature, *Journal of Power Sources*, n°123: pp. 86–93.